Eur Spine J (2008) 17:432–438
DOI 10.1007/s00586-008-0601-5

ORIGINAL ARTICLE

The distribution of mineral density in the cervical vertebral endplates

Magdalena Müller-Gerbl · Stefan Weißer · Ulrich Linsenmeier

Received: 1 August 2006 / Revised: 5 December 2007 / Accepted: 21 December 2007 / Published online: 12 January 2008

Abstract Subsidence of various constructs into the vertebral body is a well-known complication in anterior fusion. Information on bone structure is needed, as a basis for improving these procedures. There are, however, no data available on the distribution of mineral density within vertebral endplates. In this study the regional distribution of mineralization within the cervical endplates with respect to endplate orientation (inferior and superior endplate) and level distribution (C3–C7) was examined by means of computed tomographic osteoabsorptiometry (CT-OAM). The distribution of mineralization in 80 cervical endplates of 8 spinal columns (4 male, 4 female, age range 38–62 years) in vertebrae C3–C7 was investigated by CT osteoabsorptiometry (CT-OAM). The subchondral mineralization distribution revealed considerable topographic differences within each endplate, whereby the areas of greatest density were found in the peripheral marginal zones with maxima in the posterolateral surface, whereas mineralization density was much lower in the central areas. The superior endplates showed an additional posteromedial maximum, whereas the inferior endplates showed an additional anterior mineralization maximum. Comparison of the distribution patters of inferior and superior endplates at different levels from C3 to C7 reveals a uniform increase of mineralization in the anterior portions from cranial to caudal. The mineralization distribution showed characteristic reproducible patterns. The maximal values occurred in the posterolateral parts, and can thus be considered a morphological substrate of high long-term loading. This can serve as a basis for improved prosthesis design and the anchorage point for various fusion techniques.

Keywords Mineral density · Cervical spine-endplate · CT-osteoabsorptiometry (CT-OAM)

M. Müller-Gerbl (✉)
Anatomical Institute, University of Basel,
Pestalozzistrasse 20, 4056 Basel, Switzerland
e-mail: m.mueller-gerbl@unibas.ch

S. Weißer
Anatomical Institute, University of Munich,
Pettenkoferstrasse 11, 80336 Munich, Germany

U. Linsenmeier
Department of Clinical Radiology,
Ludwig-Maximilians University, Munich, Germany

Introduction

The vertebral endplate is a thin layer of dense subchondral bone adjacent to the intervertebral disc, as well as the underlying cancellous bone. Collectively they are known as preferential locations prone to fracture in the vertebral body [3, 7, 8, 38]. This is the site where subsidence occurs with interbody fusion constructs in adjacent endplates [2, 5, 9, 10, 17, 37]. Nevertheless, whereas the cancellous bone of the vertebra has been subject to numerous studies [11, 18–20, 26, 27], the literature concerning the subchondral vertebral endplate and its attached trabecular architecture is comparatively sparse. The vertebral endplate serves the dual role of containing the adjacent disc and evenly distributing applied loads to the underlying cancellous bone and the cortex of the vertebra [4]. Together with its overlying cartilage layer, the endplate also serves as a semipermeable interface that allows the transfer of water and solutes, but prevents the loss of large proteoglycan molecules from the disc [4]. Besides providing secure anchorage for the collagen fibres of the intervertebral disc,

the endplate plays a major biological role in the integration of bone grafts used in intervertebral arthrodesis [32].

Recent studies have shown that there are significant regional variations in thickness within the lumbar vertebral endplate, with thicker bone found under the annulus than adjacent to the nucleus [34]. Beyond that, Roberts also found a positive correlation between the thickness of the subchondral vertebral bone and the proteoglycan content of the adjacent disc, particularly in the region of the nucleus, possibly the result of a remodelling process, whereby the endplate responds to a greater hydrostatic pressure in discs with higher proteoglycan content [34]. Pitzen and Schmitz [30, 36] have found that the anterior and medial aspects of cervical superior endplates are significantly thinner than the lateral and posterior parts.

The local material properties of the endplate also show a significant spatial distribution. In the lumbar spine, the posterolateral regions are significantly stronger and stiffer than the middle regions [5, 12, 16]. Oxland [28] demonstrated that the lower lumbar vertebra endplates have a significant influence on compression stiffness. Li [13] described similar findings in the cervical spine. Here as well, the posterior region of the superior endplate and the lateral regions of the inferior endplate were stronger and more rigid than other regions across the endplate surface. A study by Wenger et al. [39] in the lumbar spine indicated that bone density also exhibits regional variations.

The distribution of subchondral mineralization within a joint surface is known to reflect the long-term distribution of stress over an articular surface, thus representing a morphological parameter of long-term stress distribution. By means of CT osteoabsorptiometry (CT-OAM), these distribution patterns can be displayed both in vitro and in vivo [21–25]. In contrast to the usual methods of CT densitometry, which deal with the calculation of an absolute value for bone density, CT-OAM is a procedure for demonstrating differences in relative concentration within a joint surface. Previous results indicated the regularity of the distribution of subchondral bone density as a function of the passing demands made upon a joint and thus, the resulting densitograms (distribution patterns of mineralization) can be regarded as the expression of the long-term effective stress distribution within a joint surface.

To gain insights into the long-term loading patterns within the cervical endplates, we applied CT-OAM to investigate whether regional variations apply within an endplate, between superior and inferior endplates and between the different cervical levels. Finally the distribution patterns of mineralization will be compared with distribution patterns of strength from studies of other authors to find out if correlation between both parameters exists.

Materials and methods

A total of 80 endplates (40 inferior and 40 superior endplates) from 8 spinal columns from preparations of the Anatomical Institute of Ludwig Maximilian University in Munich were used in this study. The age distribution of the spinal columns included in study evaluation was from 38 to 62 years (8 spinal columns, 4 male, 4 female) with an average age of 51.1 years (Table 1.) The exclusion criterion applied was that the donors be as young as possible and show minimum or no degenerative changes. To this end, the selected spinal columns were X-rayed using a Siemens system in posterior–anterior and lateral images to further exclude severe degenerative changes. Criteria for inclusion were a good delineation of vertebrae, large disc spaces of approximately uniform height, no osteophytes, and no endplate compression fractures.

CT osteoabsorptiometry (CT-OAM, [21–25], Fig. 1): After the intervertebral discs and ligamental structures were sharply dissected and removed, the spinal columns were separated into individual vertebrae. Then CT data were recorded (Siemens Somatom S4, Erlangen) with a layer thickness of 1 mm for each individual vertebra in coronal slices. Then the program "Analyze" was used to reconstruct the vertebrae in three dimensions (3D) with views of the articular surfaces of the inferior and superior endplates of the vertebrae. In a subsequent editing step, virtual endplates were cut out to match the superior and inferior plates of the vertebrae, then reconstructed using a maximum intensity projection (the densest value in the subchondral plate is projected onto the surface) with rotation data identical to those used to generate the overall view, whereupon the density distribution is converted to false colours. The density range from <200 HU to >1200 HU is divided into 10 grey value stages of 100 Houndfield units (HU) each. Black was used to represent the areas >1200 HU, followed in descending order by dark red, light red, yellow, green and dark blue. The result was a cartographic view of mineralization density distribution within a given endplate, which was then superimposed on

Table 1 Data on material used

ID	Age (years)	Weight (kg)	Size (cm)	Sex
90/99	44	43	167	Female
100/94	57	–	–	Female
108/99	58	42	160	Female
44/99	62	60	180	Female
27/00	38	80	178	Male
91/96	40	–	190	Male
85/99	54	71	174	Male
99/99	56	71	184	Male

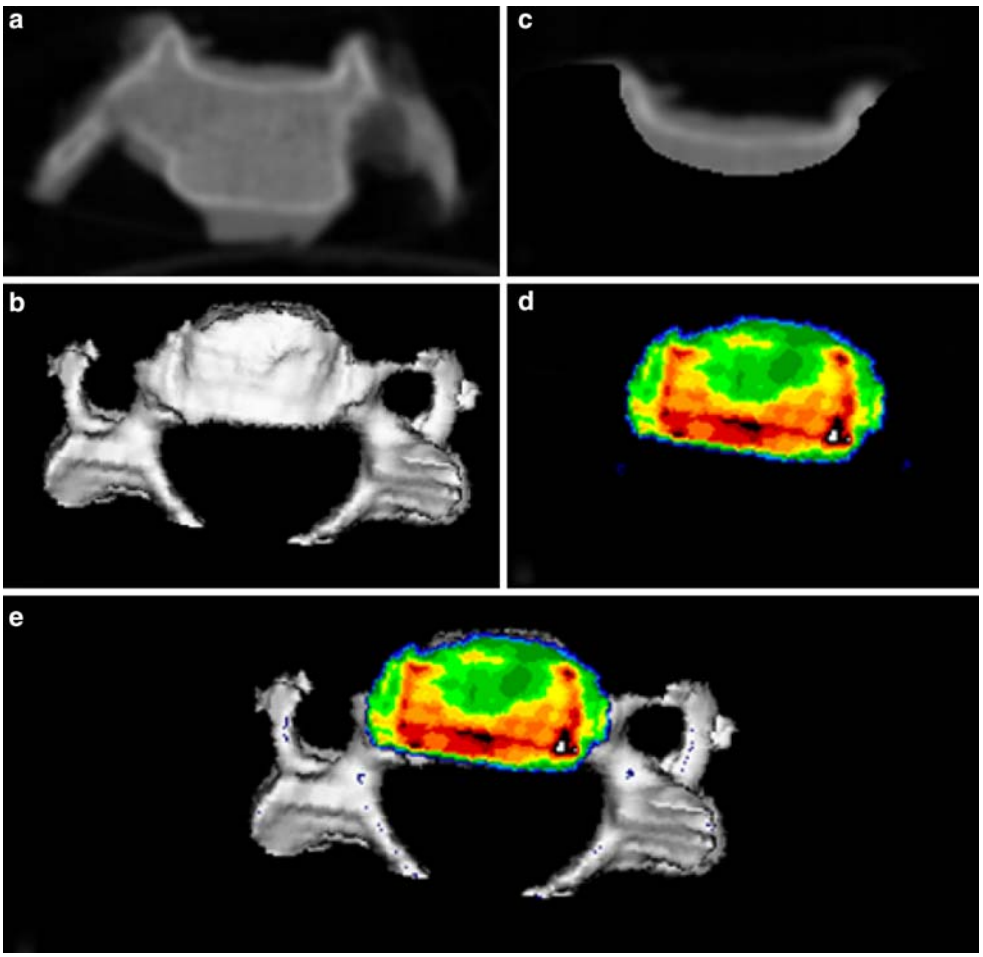

Fig. 1 CT osteoabsorptiometry, with which the densitograms were generated, **a** original CT image (coronal slice), **b** 3D reconstruction of vertebral body, **c** cut out of subchondral endplate, **d** MIP reconstruction of endplate, **e** full view (top view of a superior endplate)

the overall view of the vertebra. The resulting images (densitograms) served as a basis for further evaluation.

To quantify the distribution patterns, a 30 × 30 unit grid was projected onto each endplate densitogram. The grid was positioned in each case in tangential contact with the outermost points on the endplate on all sides. The number of units (30 × 30) was also kept the same in order to standardize the coordinates for both smaller and larger endplates. The coordinates of the focal point of each maximum were then read off (Fig. 2). Then a summary image of the maximum localization was generated in the form of a point cluster from the coordinates of all endplates investigated, separately for the inferior and superior endplates. Additionally summary images were created for the different levels C3–C7, separately for the inferior and superior endplates. Statistical analysis of these data was performed with the chi-square test and the level of significance was $P < 0.05$.

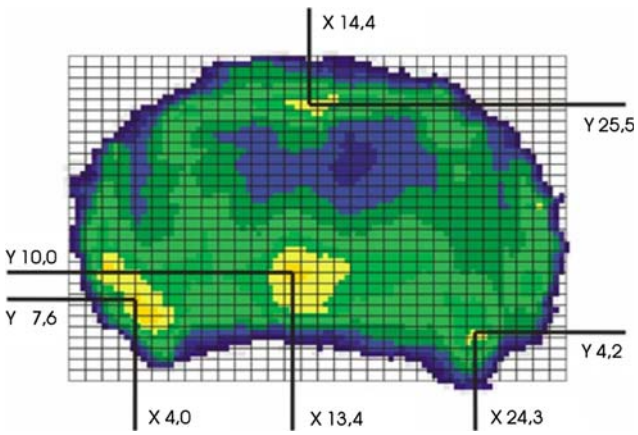

Fig. 2 Localization of the maxima using a standardized grid

Results

1. *Regional variations of mineral density within an endplate*

The subchondral mineralization distribution (Fig. 3) revealed considerable variation within each endplate. The

HU values varied between 200 and 1200 HU within an endplate.

In all of the endplates investigated, the areas of greatest density were found in the marginal zones, whereas mineralization density was much lower in the central areas. These differences were highly significant ($P < 0.0001$). No significant differences were observed for any of the endplates between right and left areas. Areas of greater and lesser density could also be identified within the highly mineralized marginal areas, depending on localization. The zones of greatest density, in both the inferior and superior endplates, were localized over wide areas of the posterolateral parts. Emerging from these areas, a somewhat less dense zone extended into the lateral parts and anteriorly (Fig. 3).

2. *Variations of mineral density with respect to endplate orientation (superior versus inferior endplate)*

The superior endplates showed an additional posteromedial maximum, the inferior endplates generally exhibited an additional anterior mineralization maximum (Fig. 4). Whereas the differences between posterior and anterior parts were highly significant in the superior endplates ($P < 0.0001$), no significant differences were found in the inferior endplates ($P = 0.076$).

3. *Variations of mineral density with respect to the level (C3–C7)*

Comparison of the distribution patterns of inferior and superior endplates at different levels from C3 to C7 (Fig. 5) revealed a uniform increase of mineralization in the anterior portions from cranial to caudal, although in all cervical endplates the largest and most extensive density maxima occurred in the posterior and posterolateral locations.

Discussion

The present study clearly demonstrated considerable topographic differences in mineralization within a given endplate. The zones of greatest mineralization are found in

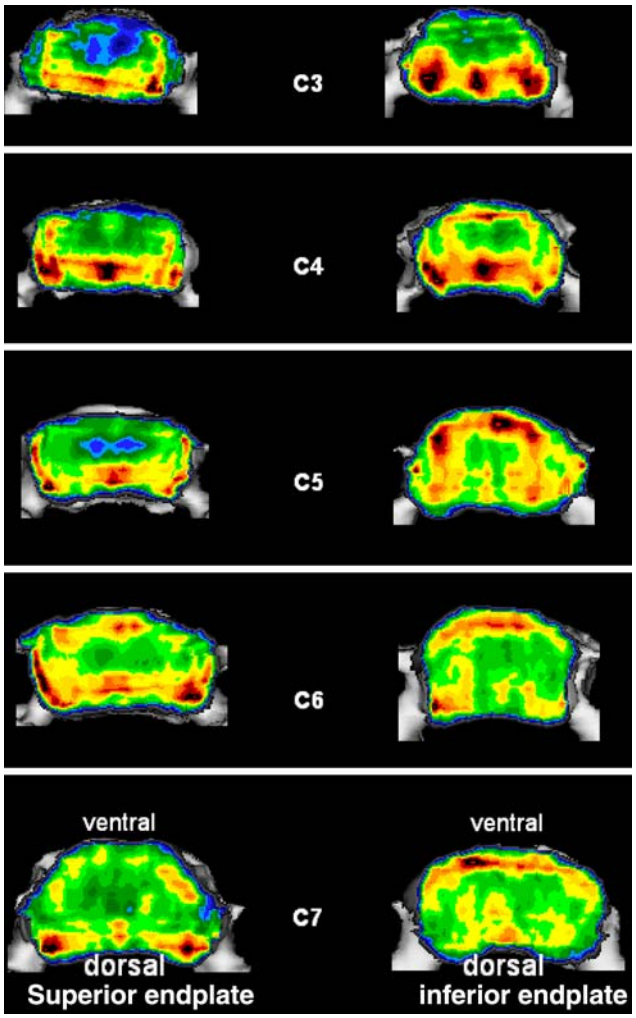

Fig. 3 Example of the mineralization distribution in the inferior and superior endplates in the cervical spine of a 38-year-old man

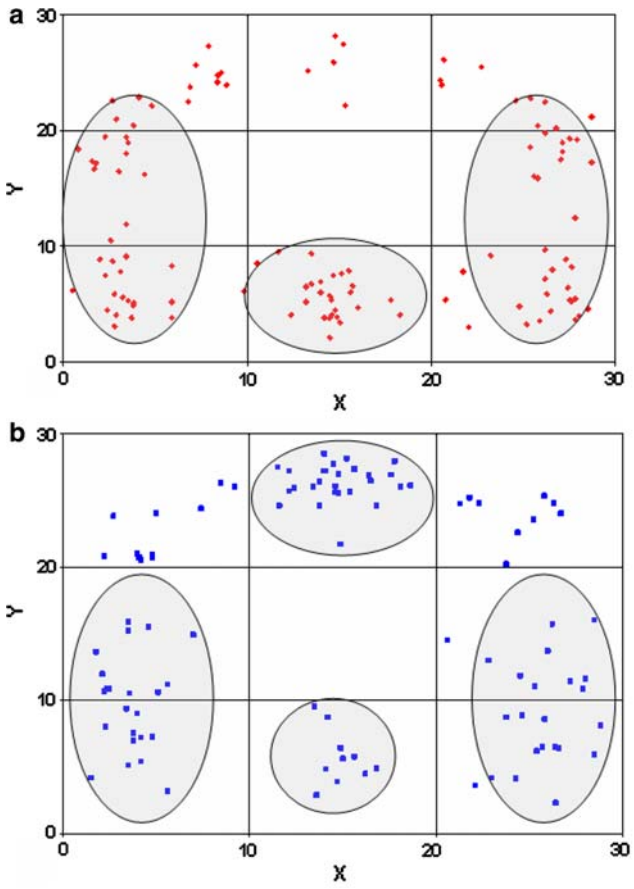

Fig. 4 Visualization of the maxima in all specimens as a point cluster done separately for the cervical superior (**a**) and inferior endplates (**b**)

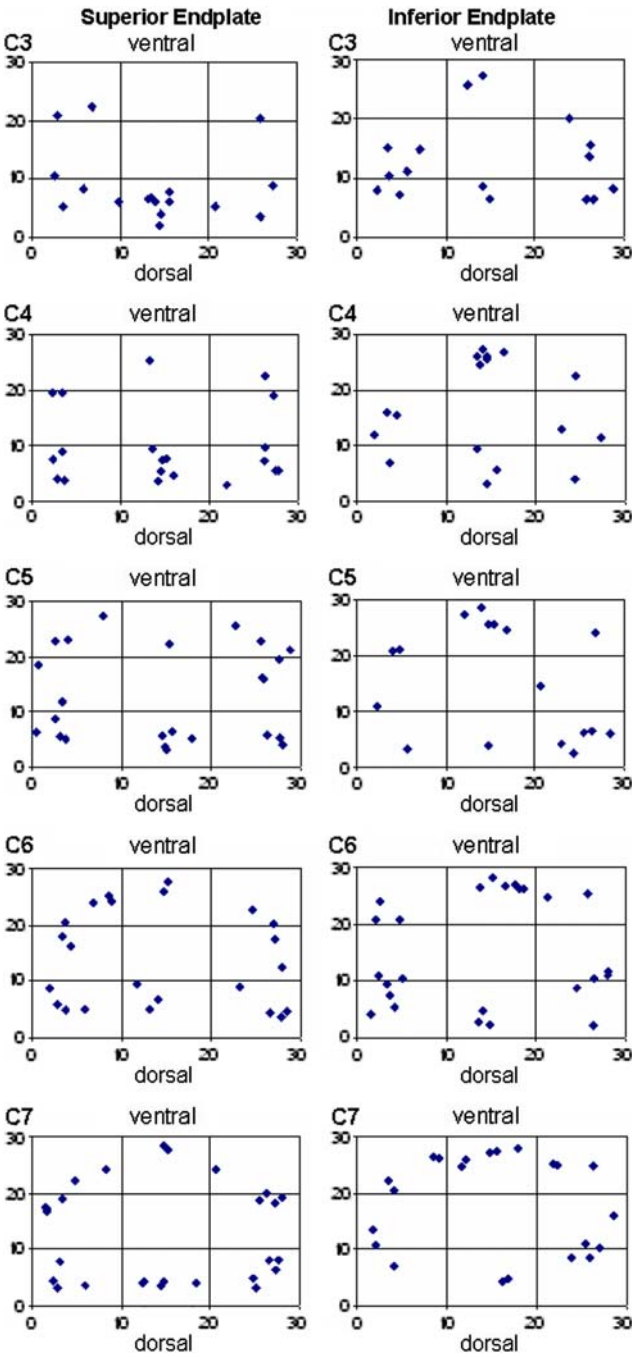

Fig. 5 Visualization of the maxima in all specimens as a point cluster for each vertebral level separately for the cervical superior and inferior endplates

the posterolateral area, with somewhat less dense areas in the lateral area, regardless of the level of the vertebral segment and regardless of whether a superior or inferior endplate is considered. Additionally, these zones of greatest density are not restricted to the marginal strip, but show a wide dorsal distribution in particular, in some cases extending anteriorly to cover over half of the vertebra. The central and anterior zone with the exception of the anterior margin, always show much lower levels of mineralization. To our knowledge, this may be the first time that it has been demonstrated that the level of mineralization within a given endplate also shows considerable regional variation. Similar findings have been described in recent years by other authors regarding thickness distribution of the subchondral endplates. In the lumbar endplates, the thickness of the plates is greater at the margins than in the central region [3, 34]. In addition, the cartilaginous endplate shows a similar thickness distribution pattern [35]. More recent publications on the thickness distribution of cervical endplates [29, 30, 36] describe a distribution pattern similar to that occurs in lumbar endplates. Lim [14] also reports that regional thickness variations are present, albeit generating only an endplate average of all the measurements he performed (nine measurement points per endplate).

Comparison of the thickness distribution in endplates with the density distribution displayed in this study demonstrates a correlation of the distribution patterns and supports the conclusion that both the thickness and the density can be considered morphological parameters of long-term load within the endplates. The further conclusion follows that, in addition to these structural parameters, material characteristics such as strength and rigidity would also show variations of distribution. Indentation test studies [5, 6, 12, 16, 28] are consistent with these findings and also show that the local material properties of the lumbar endplates demonstrate a significant spatial dependence. These authors have shown that strength and stiffness of the endplate are highest posterolaterally and lowest in the center of the endplate. Indentation tests in the cervical endplates by Li et al. [13] showed that the posterior region of the superior endplate and the lateral regions of the inferior endplate were stronger and more rigid than any other region across the endplate surface in an endplate-intact group. In the endplate-removed group, however, the posterior region of the superior endplate and the posterolateral regions of the inferior endplate were stronger and more rigid. Comparing the distribution patterns of the structural parameters of the endplate, such as thickness or mineralization show a high correlation with the distribution of material properties such as strength and rigidity. This results in a uniform, correlating pattern for all, suggesting the conclusion that all parameters reflect the long-term load of the endplates.

A comparison of the mineralization of inferior and superior endplates shows the zones of greatest density in both within the posterolateral part with a lateral extension towards the front. Whereas the superior endplates also feature a zone of higher density in the posteromedial area, the inferior endplates show an additional maximum in the anteromedial area, indicating that the superior and inferior

endplates are subjected to different anterior and posterior loading.

Comparing the mineralization distribution at different segment levels reveals a tendential shift in the maxima in the superior endplates in particular. Whereas in segments C3 and C4 the maxima are localized solely in the posterolateral and posteromedial areas, segments C5–C7 gradually begin to show maximal density in the anterolateral and anteromedial areas. This indicates, as other publications on the orientation of the vertebral joints have demonstrated [1, 33], that the cervical spine between C2 and C7 is not uniformly loaded, but rather that considerable differences apply depending on the vertebral segment.

According to a finite element model used by Polikeit et al. [31], the distinction between failure and success of interbody fusion is influenced by a number of parameters. They showed that cage insertion changes the overall load transfer of static loads. In fact, the material properties of the cancellous bone and the endplate were found to be more important factors preventing subsidence and interbody instrumentation failure than either the cage material or the loading conditions. Polikeit et al. concluded that cages should be designed such that they rely on the strong peripheral parts of the endplate to reduce the risk of subsidence.

Similar considerations are also relevant to the design of intervertebral disc prostheses [15] in choosing the optimal anchoring points of the cervical vertebral bodies.

Both the present study and those of other authors make it clear that there are regional variations of both structural parameters and material properties, and that these patterns correlate and therefore reflect the loading distribution on the endplates. Each of these parameters, taken separately, can be considered a parameter for stress distribution.

In previous studies [21–23] for validation of the CT-OAM method we could show in several compare-and-contrast studies that CT OAM produces the same results as those obtained by conventional X-ray densitometry both displaying the distribution of subchondral mineralization.

One advantage of the mineralization distribution method we used is that the mineralization distribution is displayed continuously over the entire endplate, whereas measurement of other parameters such as thickness, strength and rigidity, can only be realized at isolated points. A further advantage is that this method can be applied to living patients, making it possible to image the mineralization distribution in individual patients.

In clinical applications, the data from this study of subchondral mineralization distribution can serve as a basis, for instance in optimization of interbody fusion methods. The same applies to the design and anchorage of intervertebral disc prostheses.

Conclusions

The mineral density of the cervical spine endplate showed characteristic reproducible density patterns. The marginal areas are significantly higher mineralized than the central part. The maximal values occurred in the posterolateral parts. The inferior endplates generally showed an additional anterior mineralization maximum. Whereas in segments C3 and C4 the maxima are localized solely in the posterolateral and posteromedial areas, segments C5–C7 gradually begin to show maximal density in the anterolateral and anteromedial areas.

References

1. Bogduk N, Mercer S (2000) Biomechanics of the cervical spine. I: Normal kinematics. Clin Biomech 15:633–648
2. Diedrich O, Perlick L, Schmitt O, Kraft CN (2001) Radiographic characteristics on conventional radiographs after posterior lumbar interbody fusion: comparative study between radiotranslucent and radiopaque cages. J Spinal Disord 14:522–532
3. Edwards WT, Zheng Y, Ferrara LA, Yuan HA (2001) Structural features and thickness of the vertebral cortex in the thoracolumbar spine. Spine 26:218–225
4. Ferguson SJ, Steffen T (2003) Biomechanics of the aging spine. Eur Spine J 12(Suppl 2):S97–S103
5. Grant JP, Oxland TR, Dvorak MF (2001) Mapping the structural properties of the lumbosacral vertebral endplates. Spine 26:889–896
6. Grant JP, Oxland TR, Dvorak MF, Fisher CG (2002) The effects of bone density and disc degeneration on the structural property distributions in the lower lumbar vertebral endplates. J Orthop Res 20:1115–1120
7. Holmes A, Hukins D, Freemont A (1993) End-plate displacement during compression of lumbar vertebra-disc-vertebra segments and the mechanism of failure. Spine 18:128–135
8. Ikeuchi M, Yamamoto H, Shibata T, Otani M (2001) Mechanical augmentation of the vertebral body by calcium phosphate cement injection. J Orthop Sci 6:39–45
9. Jost B, Cripton P, Lund T, Oxland TR, Lippuner K, Jaeger P, Nolte LP (1998) Compressive strength of interbody cages in the lumbar spine: the effect of cage shape, posterior instrumentation and bone density. Eur Spine J 7:132–141
10. Kettler A, Wilke H-J, Dietl R, Krammer M, Lumenta C, Claes L (2000) Stabilizing effect of posterior lumbar interbody fusion cages before and after cyclic loading. J Neurosurg 92(1 Suppl):87–92
11. Kothari M, Keaveny TM, Lin JC, Newitt DC, Genant HK (1998) Impact of spatial resolution on the prediction of trabecular architecture parameters. Bone 22:437–443
12. Kumar A, Doherty B (1993) Biomechanical testing of vertebral endplates strength: a cadaver study. NASS 8th Annual Meeting, San Diego
13. Li JY, Zhu QA, Zhao WD, Lin LJ, Zhang MC, Huang WH (2003) Role of the biomechanical property of the endplate in anterior cervical fusion. Di Yi Jun Yi Da Xue Xue Bao 23(5):402–408
14. Lim TH, Kwon H, Jeon CH, Kim JG, Sokolowski M, Natarajan R, An HS, Andersson GB (2001) Effect of endplate conditions and bone mineral density on the compressive strength of the graft-endplate interface in anterior cervical spine fusion. Spine 26:951–956

15. Link HD, McAfee PC, Pimenta L (2004) Choosing a cervical disc replacement. Spine J 4(Suppl):294S–302S
16. Lowe TG, Shukor H, Wilson LA, ÓBrien MF, Smith DAB, Diekmann MJ, Trommeter J (2004) A biomechanical study of regional endplate strength and cage morphology as it relates to structural interbody support. Spine 29:2389–2394
17. McAfee P (1999) Interbody fusion cages in reconstructive operations on the spine. J Bone Joint Surg Am 81:859–880
18. Millard J, Augart P, Link T, Kothari M, Newitt DC, Genant HK, Majumdar S (1998) Power spectral analysis of vertebral trabecular bone structure from radiographs: orientation dependence and correlation with bone mineral density and mechanical properties. Calcif Tissue Int 63:482–489
19. Mosekilde L (1993) Vertebral structure and strength in vivo and in vitro. Calcif Tissue Int 53(Suppl 1):S121–S125, discussion S125–S126
20. Mosekilde L, Mosekilde L, Danielsen CC (1987) Biomechanical competence of vertebral trabecular bone in relation to ash density and age in normal individuals. Bone 8:79–85
21. Muller-Gerbl M (1998) The subchondral bone plate. Adv Anat Embryol Cell Biol 141(III–XI):1–134
22. Muller-Gerbl M, Putz R, Hodapp N, Schulte E, Wimmer B (1989) Computed tomography-osteoabsorptiometry for assessing the density distribution of subchondral bone as a measure of long-term mechanical adaptation in individual joints. Skeletal Radiol 18:507–512
23. Muller-Gerbl M, Putz R, Hodapp N, Schulte E, Wimmer B (1990) Computed tomography-osteoabsorptiometry: a method of assessing the mechanical condition of the major joints in a living subject. Clin Biomech 5:193–198
24. Muller-Gerbl M, Putz R, Hodapp N, Schulte E, Wimmer B (1990) Demonstration of subchondral density pattern using CT-osteoabsorptiometry (CT-OAM) for the assessment of individual joint stress in live patients. Z Orthop Ihre Grenzgeb 128:128–133
25. Muller-Gerbl M, Putz R, Kenn R (1992) Demonstration of subchondral bone density patterns by three-dimensional CT osteoabsorptiometry as a noninvasive method for in vivo assessment of individual long-term stresses in joints. J Bone Miner Res 2:S411–S418
26. Odgaard A (1997) Three-dimensional methods for quantification of cancellous bone architecture. Bone 20:315–328
27. Overaker D, Langrana NA, Cuitino A (1999) Finite element analysis of vertebral body mechanics with a nonlinear microstructural model for the trabecular core. J Biomech Eng 121:542–550
28. Oxland TR, Grant JP, Dvorak MF, Fisher CG (2003) Effects of endplate removal on the structural properties of the lower lumbar vertebral bodies. Spine 28:771–777
29. Panjabi MM, Chen NC, Shin EK, Wang J-L (2001) The cortical shell architecture of human cervical vertebral bodies. Spine 26:2478–2484
30. Pitzen T, Schmitz B, Georg T, Barbier D, Beuter T, Steudel WI, Reith W (2004) Variation of endplate thickness in the cervical spine. Eur Spine J 13:235–240
31. Polikeit A, Ferguson SJ, Nolte LP, Orr TE (2003) The importance of the endplate for interbody cages in the lumbar spine. Eur Spine J 12:556–561
32. Porto Filho MR, Pastorello MT, Defino HL (2005) Experimental study of the participation of the vertebral endplate in the integration of bone grafts. Eur Spine J 14:965–970
33. Putz R (1981) Funktionelle Anatomie der Halswirbelsäule. Normale und Pathologische Anatomie 43. Thieme, Stuttgart
34. Roberts S, McCall IW, Menage J, Haddaway MJ, Eisenstein SM (1997) Does the thickness of the vertebral subchondral bone reflect the composition of the intervertebral disc? Eur Spine J 6:385–389
35. Roberts S, Menage J, Urban JPG (1989) Biochemical and structural properties of the cartilage end-plate and its relation to the intervertebral disc. Spine 14:166–174
36. Schmitz B, Pitzen T, Beuter T, Steudel WI, Reith W (2004) Regional variations in the thickness of cervical spine endplates as measured by computed tomography. Acta Radiol 45:53–58
37. Steffen T, Tsantrizos A, Aebi M (2000) Effect of implant design and endplate preparation on the compressive strength of interbody fusion constructs. Spine 25:1077–1084
38. van Dieen J, Kingma I, Meijer R, Hänsel L, Huiskes R (2001) Stress distribution changes in bovine vertebrae just below the endplate after sustained loading. Clin Biomech 16(Suppl 1):S135–S142
39. Wenger K, Pross A, Wilke H-J, Gossee F, Vahldiek M, Claes LE (1999) Bone mineral density of the vertebral endplate: an in vitro comparison of normals, degeneratives and osteoporotics. 26th Annual Meeting, ISSLS, Kona